Trivalent Lanthanide Chalcogenolates: Synthesis, Structure, and Thermolysis Chemistry

Jongseong Lee, Meggan Brewer, M. Berardini, and J. G. Brennan*

Department of Chemistry, Rutgers, The State University of New Jersey, Piscataway, New Jersey 08855-0939

Received January 12, 1995[⊗]

Lanthanide–mercury amalgams react with diphenyl diselenide to form tris(benzeneselenolates) that can be isolated as the crystalline pyridine coordination complexes $(pyridine)_3Ln(SePh)_3$ (Ln = Ho (**1**), Tm (**2**), Yb (**3**)). The structure of **2** was established by low temperature single crystal X-ray diffraction. The complex is dimeric in the solid state, with 7-coordinate metal centers connected by a pair of μ_2-(benzeneselenolate) ligands. Thermal decomposition of the selenolates gives a variety of solid state metal selenides: **1** gives HoSe, $HoSe_2$, and Ph_2Se; **2** gives Tm_2Se_3 and Ph_2Se; **3** gives Yb_2Se_3 and Ph_2Se. Trivalent thiolates can also be prepared by this amalgam reaction. For comparison, the structure of $Yb(SPh)_3(pyridine)_3$ (**4**) was also determined—**4** is a monomeric *mer*-octahedral compound with inequivalent Yb–S bonds. Both **3** and **4** have an intense visible chalcogen-to-ytterbium charge transfer absorption band. Crystal data (Mo Kα, 153(2) K) are as follows. **2**: Triclinic space group $P\bar{1}$, a = 10.435(2) Å, b = 12.748(2) Å, c = 14.453(2) Å, α = 69.85(2)°, β = 80.71(2)°, and γ = 69.03(2)°. **4**: Triclinic space group $P\bar{1}$, a = 9.836(10) Å, b = 11.304(14) Å, c = 16.202(11) Å, α = 80.70°, β = 77.91(7)°, and γ = 68.34(9)°.

Introduction

There are both fundamental and applied motivations for studying the coordination chemistry of lanthanides (Ln) bound to anionic thiolate, selenolate, or tellurolate (chalcogenolate) ligands. Fundamentally, the nature of the bonding between these electropositive metal ions and the heavier, less electronegative chalcogenolates is relatively unexplored. While bonding in the solid state lanthanide chalcogenide compounds has long been discussed in terms of considerable covalent bonding character,[1] little is known about the nature of molecular lanthanide–chalcogen bonds. Because the lanthanide valence 4f shell is less radially extended than filled 5s and 5p shells, ligands bound to lanthanide ions experience a spherical electrostatic potential. Lanthanide chemistry is dominated by "hard", nonpolarizable donor ligands which optimize nondirectional, electrostatic metal–ligand interactions.

Early attempts to study molecular lanthanide–chalcogenolate bonds were discouraging—"homoleptic" lanthanide thiolates were reported to be insoluble in organic solvents.[2] Application of the pentamethylcyclopentadienyl[3] (Cp*) ligand to lanthanide–chalcogen chemistry led to the preparation of soluble, crystalline lanthanide thiolates, as well as lanthanide complexes with single bonds to the heavier chalcogens Se and Te, which until then were considered too electropositive to form stable complexes. As recently as 1990, the same idea of using sterically demanding, highly electronegative heteroallylic ancillary ligands to stabilize lanthanide–chalcogen bonds was being pursued.[4] Unfortunately, in both heteroallyl and Cp* compounds, the interpretation of bond geometries about the chalcogen atom was hampered by the distinct possibility that intramolecular ligand–ligand repulsive interactions were determining molecular structure.

In the past few years there has been a surge of interest in preparing lanthanide complexes with chalcogenolates as the only anions.[5] This synthetic effort is motivated by the expanding interest in using lanthanides to dope semiconductors,[6] as well as to dope sulfur- and selenium-based fiber optic and laser materials.[7] In both applications it is the sharp optical f–f emissions of the lanthanide elements that are useful. The advantages of using molecular lanthanide chalcogenolate complexes to dope these chalcogenide materials are 2-fold. First, molecular chalcogenolates decompose to deliver LnE_x. The resultant lanthanide coordination sphere in the chalcogenide matrix contains only one type of chalcogen atom, giving rise to optimally sharp optical properties. More importantly, the lanthanide is directly bound to the chalcogenide matrix. The

[⊗] Abstract published in *Advance ACS Abstracts,* May 15, 1995.

(1) (a) Gerth, G.; Kienle, P.; Luchner, K. *Phys. Lett. A* **1968**, *27*, 557–558. (b) Eatough, N. L.; Hall, H. T. *Inorg. Chem.* **1970**, *9*, 417–418. (c) Dagys, R. S.; Anisimov, F. G. *Sov. Phys. Solid State* **1984**, *26*, 547–8 . (d) Wachter, P. *Crit. Rev. Solid State* **1972**, *3*, 189–241. (e) Byrom, E.; Ellis, D. E.; Freeman, A. J. *Phys. Rev. B* **1976**, *14*, 3558–3568. (f) Zhukov, V. P.; Gubanov, V. A.; Weber, J. *J. Chem. Phys. Solids* **1981**, *42*, 631–639.

(2) Gharia, K. S.; Singh, M.; Mathur, S.; Roy, R.; Sankhla, B. S. *Synth. React. Inorg. Met-Org. Chem.* **1982**, *12*, 337–345.

(3) (a) Schumann, H.; Albrecht, I.; Hahn, E. *Angew. Chem., Int. Ed. Engl.* **1985**, *24*, 985–986. (b) Berg, D.; Burns, C.; Andersen, R. A.; Zalkin, A. *Organometallics* **1988**, *8*, 1858–1863. (c) Berg, D. J.; Burns, C.; Andersen, R. A.; Zalkin, A. *Organometallics* **1989**, *8*, 1865–1870. (d) Zalkin, A.; Berg, D. J. *Acta Crystallogr.* **1988**, *44C*, 1488–1489. (e) Evans, W.; Grate, J. W.; Bloom, I.; Hunter, W. E.; Atwood, J. L. *J. Am. Chem. Soc.* **1985**, *107*, 405–409. (f) Evans, W; Rabe, G.; Ziller, J.; Doedens, R. *Inorg. Chem.* **1994**, *33*, 2719–2726.

(4) Welder, M.; Noltemeyer, M.; Pieper, U.; Schmidt, H.; Stalke, D.; Edelmann, F. *Angew. Chem., Int. Ed. Engl.* **1990**, *29*, 894.

(5) (a) Strzelecki, A. R.; Timinski, P. A.; Hesel, B. A.; Bianconi, P. A. *J. Am. Chem. Soc.* **1992**, *114*, 3159–3160. (b) Cary, D. R.; Arnold, J. *J. Am. Chem. Soc.* **1993**, *115* 2520–2521. (c) Berardini, M.; Emge, T.; Brennan, J. G. *J. Chem. Soc. Chem. Comm* **1993**, 1537–1538. (d) Berardini, M.; Emge, T.; Brennan, J. G. *J. Am. Chem. Soc.* **1993**, *115*, 8501–8502. (e) Khasnis, D. V.; Lee, J.; Brewer, M.; Emge, T. J.; Brennan, J. G. *J. Am. Chem. Soc.* **1994**, *116*, 7129–7133. (f) Brewer, M.; Khasnis, D.; Buretea, M.; Berardini, M.; Emge, T. J.; Brennan, J. G. *Inorg. Chem.* **1994**, *33*, 2743–2747. (g) Carey, D. R. Arnold, J. *Inorg. Chem.* **1994**, *33*, 1791. (h) Mashima, K.; Nakayama, Y.; Kanehisa, N.; Kai, Y.; Nakamura, A. *J. Chem. Soc., Chem. Commun.* **1993**, 1847–1848. (i) Strzelecki, A. R.; Likar, C.; Hesel, B. A.; Utz, T.; Lin, M. C.; Bianconi, P. A. *Inorg. Chem.* **1994**, *33*, 5188. (j) Mashima, K.; Nakayama, Y.; Fukumoto, H.; Kanehisa, N.; Kai, Y.; Nakamura, A. *J. Chem. Soc., Chem. Commun.* **1994**, 2523–2524. (k) Tatsumi, K.; Amemiya, T.; Kawaguchi, H.; Tani, K. *J. Chem. Soc., Chem. Commun.* **1993**, 773–774. (l) Cetinkaya, B.; Hitchcock, P. B.; Lappert, M. F.; Smith, R. G. *J. Chem. Soc., Chem. Commun.* **1992**, 932–933. (m) Cary, D.; Ball, G.; Arnold, J. *J. Am. Chem. Soc.* **1995**, *117*, 3492.

0020-1669/95/1334-3215$09.00/0

utilityof these materials depends on the efficiency of energy transfer from the excited chalcogen matrix to the lanthanide element, and direct lanthanide−matrix bonds serve to optimize the process. Second, molecular lanthanide chalcogenolates can be used to deliver uniform concentrations of Ln ions at relatively low temperatures—the tellurolates decompose below 100 °C and the thiolates decompose below 400 °C. Such low temperatures are important when the desired product is a metastable solid (i.e. a fiber optic glass that would crystallize at elevated temperatures). For both reasons, molecular chalcogenolate complexes are attractive Ln sources, especially when compared to the conventional lanthanide halide or carboxylate sources.

Ln(III) chalcogenolate chemistry is particularly underdeveloped due to the relative inability of these more electropositive ligands to stabilize higher metal oxidation states. In trivalent chemistry, the increased metal charge stabilizes metal based orbitals, possibly to the point where metal−ligand orbital overlap could have a measurable effect on metal−ligand bonding. While the valence metal 4f orbitals are too radially contracted (relative to filled 5s and 5p orbitals) to overlap with ligand based orbitals, the lanthanide do have unfilled 5d and 6p orbitals available for covalent interactions.[1] This paper presents our initial efforts to outline the chemistry of trivalent lanthanide phenylchalcogenolates. We use lanthanide−mercury amalgams to reduce diphenyl dichalcogenides and produce high yields of $Ln(EPh)_3$, (E = S, Se) and we show that the selenolate compounds decompose to deliver a variety of solid state $LnSe_x$ phases.

Experimental Section

General Data. All syntheses were carried out under ultrapure nitrogen (JWS), using conventional drybox or Schlenk techniques. Solvents (Fisher) were refluxed continuously over molten alkali metals or sodium/benzophenone and collected immediately prior to use. Anhydrous pyridine (Aldrich) was purchased and refluxed over KOH. PhSeSePh and PhSSPh were purchased from either Aldrich or Strem and recrystallized from hexane. Tm, Ho, Yb, and Hg were purchased from Strem. Melting points were taken in sealed capillaries, and are uncorrected. IR spectra were taken on a Mattus Cygnus 100 FTIR spectrometer, and recorded from 4000−450 cm^{-1}, as a Nujol mull. Electronic spectra were recorded on a Varian DMS 100S spectrometer with the samples in a 0.10 mm quartz cell attached to a Teflon stopcock. Elemental analyses were preformed by Quantitative Technologies, Inc. (Salem, NJ). NMR Spectra were obtained on either a Varian Gemini 200 MHz or Varian 400 MHz NMR spectrometer at 23 °C, and are reported in δ (ppm). Powder diffraction data were obtained from SCINTAG PAD V diffractometer and Cu Kα radiation.

$(pyridine)_3Ho(SePh)_3$ (1). Ho (0.66 g, 4.0 mmol), diphenyl diselenide (1.87 g, 5.99 mmol) and Hg (1.2 g, 6.0 mmol) were added to pyridine (40 mL), and the mixture was stirred for 3 days as the solution color turned yellow. The solution was filtered, concentrated to 20 mL and layered with diethyl ether (60 mL). After 1 day, peach crystals (2.70 g, 78%; mp 130−140 °C) were collected. Anal. Calcd for $C_{33}H_{30}N_3HoSe_3$: C, 45.5; H, 3.47; N, 4.83. Found: C, 43.0; H, 3.43; N, 4.46. IR: 2029 (w), 1598 (s), 1572 (s), 1466 (m), 1411 (m), 1377 (s), 1217 (s), 1152 (s), 1067 (m), 732 (m), 688 (m), 601 (m) cm^{-1}. The ^1H NMR spectrum (CD_3CN) contained broad resonances at 8.98, 7.26, and 7.11 ppm. UV: λ_{max} (ca. 1 mg/mL of pyridine) = 303 nm.

Thermolysis. 1 (550 mg) was placed in a Pyrex tube under vacuum for 1 h. The tube was then sealed and the sample temperature was raised over a period of 3 days from 50 to 300 °C, with one end of the tube kept at room temperature. Between 80 and 100 °C, a colorless liquid (pyridine) condensed in the part of the tube that was outside the furnace. Between 250 and 300 °C, dark brown diphenylselenide condensed in the cold part of the sample holder. The volatile materials were identified by ^1H NMR spectroscopy. The remaining black solid (180 mg, 100.6%) was transferred to a quartz tube that was then sealed under vacuum (10^{-7} Torr). Further heating (1000 °C, 3 days) showed no further elimination of volatile products, and an X-ray powder diffraction analysis of the final solid product revealed the presence of microcrystalline HoSe[8] and $HoSe_2$.[9]

$(pyridine)_3$ Tm$(SePh)_3$ (2). A mixture of Tm (0.68 g, 4.0 mmol), diphenyl diselenide(1.87 g, 5.99 mmol) and Hg (1.2 g, 6.0 mmol) in pyridine (40 mL) was stirred for 3 days, as the solution color turned yellow-green. The solution was filtered, concentrated (20 mL) and saturated with diethyl ether. After 1 day, yellow-green crystals (2.56 g, 76%; mp 110−120 °C) were collected. Anal. Calcd for $C_{33}H_{30}N_3Se_3Tm$: C, 45.3; H, 3.45; N, 4.80. Found: C, 44.6; H, 3.22; N, 5.24. IR: 2922 (w), 1598 (s), 1571(s), 1468 (m), 1441(m), 1378 (s), 1218 (s), 1152 (s), 1067 (m), 1021 (m), 875 (s), 732 (m), 689 (m), 624 (m), 519 (s), 467 (m), 421 (m) cm^{-1}. The ^1H NMR spectrum (CD_3CN, 25 °C) contained two sets of resonances at 12.35 ppm (7H, more than one peak is present, $w_{1/2}$ = 220 Hz) and 4.12 (5H, $w_{1/2}$ = 50 Hz) ppm) that were too broad to use for structural information. λ_{max} (ca. 1 mg/mL of pyridine): 304 nm.

Thermolysis of 2. In a fashion identical to the thermolysis of **1**, 480 mg of **2** was thermally converted into a black solid (150 mg, 95% yield), and X-ray powder diffraction revealed that Tm_2Se_3[10] was the only crystalline product present.

$(pyridine)_3Yb(SeC_6H_5)_3$ (3). Method A. Yb (0.88 g, 5.1 mmol), diphenyl diselenide (2.37 g, 7.6 mmol), and Hg (55 mg, 0.27 mmol) were stirred in THF (70 mL) for 24 h. The deep red solution was taken to dryness, and the red solid was dissolved in pyridine(15 mL) and layered with diethyl ether (60 mL). Within days large dark red crystals (3.2 g, 89%; mp 92−94 °C) had formed. Anal. Calcd for $C_{33}H_{30}N_3Se_3Yb$: C, 45.1; H, 3.44; N, 4.78. Found: C, 45.2; H, 3.43; N, 5.14. The ^1H NMR (THF-d_8) spectrum contains broad resonances ($w_{1/2}$ = 200 Hz) with maxima at 8.66, 8.35, 7.74, and 7.36 ppm. At a concentration of 20 mg/mL of **3** in deuterated THF, the OC*H*D THF resonance has a $w_{1/2}$ of 40 Hz, while the OCD_2CD*H* resonance has a $w_{1/2}$ of 40 Hz, indicating significant displacement of the pyridine ligands by the solvent. IR: 1637 (w), 1603 (s), 1588 (s), 1574 (s), 1484 (s), 1469 (s), 1440 (s), 1378 (s), 1296 (s), 1217 (m), 1069 (s), 1031 (s), 1022 (s), 1006 (s), 996 (s), 752 (s), 736 (s), 704 (s, br), 665 (s), 624 (m), 608 (m), 467 (m) cm^{-1}. The optical spectrum is concentration dependent λ_{max} (ca. 1 mg/mL pyridine): 384, 510 nm.

(6) (a) Pomrenke, G. S.; Klein, P. B.; Langer, D. W. *Rare Earth Doped Semiconductors* (MRS Symposium V. 301): Materials Research Society; Pittsburgh, PA, 1993. (b) Singer, K. E.; Rutter, P.; Praker, A. R.; Wright, A. C. *Appl. Phys. Lett.* **1994**, *64*, 707−709. (c) Swiatek, K.; Godlewski, M.; Niinisto, L.; Leskela, M. *J. Appl. Phys.* **1993**, *74*, 3442−3446. (d) Taniguchi, M.; Takahei, K. *J. Appl. Phys* **1993**, *73*, 943−947. (e) Jourdan, N.; Yamaguchi, H.; Harikoshi, Y. *Jpn. J. Appl. Phys.* **1993**, *32*, 1784−1787. (f) Kalboussi, A.; Moneger, S.; Marrakchi, G.; Guillot, G.; Lambert, B.; Guivarc'h, A. *J. Appl. Phys.* **1994**, *75*, 4171−4175. (g) Takahei, K.; Taguchi, A.; Harikoshi, Y.; Nakata, J. *J. Appl. Phys.* **1994**, *76*, 4332−4339. (h) Lozykowski, H. J.; Alshawa, A. K.; Brown, I. *J. Appl. Phys.* **1994**, *76*, 4836−4846. (i) Kimura, T.; Isshiki, H.; Ishida, H.; Yugo, S.; Saito, R.; Ikoma, T. *J. Appl. Phys.* **1994**, *76*, 3714−3719. (j) Charreire, Y.; Tolomen-Kivimaki, O.; Leskela, M.; Cortes, R.; Nykanen, E.; Soininen, P.; Niinisto, L. In *Program and Abstracts of the ICFE-2, Aug 1−6, 1994*; University of Helsinki: Helsinki, Finland. Kansikas, J., Leslela, M., Eds.; 1994; p 326. (k) Charreire, Y.; Marbeuf, A.; Tourillon, G.; Leskela, M.; Niinisto, L.; Nykanen, E.; Soininen, P.; Tolonen, O. *J. Electrochem. Soc.* **1992**, *139*, 619. (l) Charreire, Y.; Svoronos, D. R.; Ascone, I.; Tolonen, O.; Niinisto, L.; Leskela, M. *J. Electrochem. Soc.* **1993**, *140*, 2015.

(7) (a) Kanamori, T.; Terunuma, Y.; Takahashi, S.; Miyashita, T. *J. Lightwave Tech.* **1984**, *LT2*, 607. (b) Kumta, P. N.; Risbud, S. H. *Ceram. Bull.* **1990**, *69*, 1977. (c) Nishii, J.; Morimoto, S.; Yokota, R.; Yamagishi, T. *J. Non-Cryst. Solids* **1987**, *95/96*, 641−646. (d) Savage, J. A. In *Infrared Optical Materials and Their Antireflection Coatings*; Adam Hilger Ltd.: 1985; pp 79−94. (e) Nishii, J.; Morimoto, S.; Inagawa, I.; Iizuka, R.; Yamashita, T.; Yokota, R.; Yamagishi, T. *J. Non-Cryst. Solids* **1992**, *140*, 199−208. (f) Sanghara, J. S.; Busse. L. E.; Aggarwall, I. D. *J. Appl. Phys.* **1994**, *75*, 4885−4891. (g) Katsugama, T.; Matsumura, H. *J. Appl. Phys.* **1994**, *75*, 2743−2748.

(8) *Ref. Natl. Bur. Stand., Monogr. (U.S.)* **1965**, *25*, Sect 4.

(9) Wang, R.; Steinfink, H. *Inorg. Chem.* **1967**, *6*, 1658−92.

(10) Dismukes, J. P.; White, J. G. *Inorg. Chem.* **1965**, *4*, 970−3.

Method B. Diphenyl diselenide (1.56 g, 4.9 mmol) was dissolved in diethyl ether (60 mL), and sodium triethylborohydride (10 mL of a 1.0 M solution in THF, 10 mmol) was added by syringe. The yellow solution color disappeared within seconds. The colorless solution was stirred for 30 min and taken to dryness to give a white solid. Ytterbium trichloride (0.92 g, 3.3 mmol) was dissolved in THF (100 mL) and added to the sodium phenyl selenide solid. Upon mixing, a deep purple/red solution developed. The reaction was allowed to stir for 2 h, the solution was filtered, and then it was concentrated to dryness to yield a light pink solid. To this solid were added pyridine (5 mL) and diethyl ether (70 mL), and the deep red solution was filtered. After 24 h dark red crystals (0.85 g, 29%) were isolated.

Thermolysis of 3. Compound **3** was thermally decomposed in a fashion identical to the thermolysis of **1**, with the exception that the final temperature was kept at 700 °C, in an attempt to isolate metastable $YbSe_2$. In total, 810 mg of **2** was thermally converted into a black solid (250 mg, 93% yield), and X-ray powder diffraction revealed that Yb_2Se_3[11] was the only crystalline product present.

(pyridine)$_3$Yb(SPh)$_3$ (4). THF (40 mL) was added to a Schlenk containing Hg (16 mg, 0.080 mmol), Yb (600 mg, 3.47 mmol), and diphenyldisulfide (1.13 g, 5.18 mmol), and the mixture was stirred magnetically. The solution turned red within 30 min, and a red-orange solid precipitated within 1 h. After 36 h, the red mixture was taken to dryness and washed with diethyl ether. The red solid was dissolved in pyridine. The solution was filtered and layered with diethyl ether to give red crystals (1.65 g, 65%; mp 112 °C dec). The compound crystallizes with a lattice pyridine that rapidly diffuses from the lattice upon isolation. Anal. Calcd for $C_{33}H_{30}N_3S_3Yb$: C, 53.7; H, 4.10; N, 5.69. Found: C, 53.7; H, 4.18; N, 5.86. IR: 1598 (w), 1574 (w), 1452 (s), 1376 (s), 1305 (m), 1216 (w), 1168 (w), 1156 (w), 1080 (w), 1061 (w), 1035 (w), 1022 (w), 1000 (w), 967 (w), 943 (w), 733 (m), 690 (m), 623 (m) cm^{-1}. λ_{max} = 470 nm (pyridine). The ^{1}H NMR (CD_3CN, 24 °C) spectrum contained peaks at 9.18 ($w_{1/2}$ = 300 Hz), 7.85 ($w_{1/2}$ = 120 Hz), 7.49 ($w_{1/2}$ = 120 Hz), 7.27 ($w_{1/2}$ = 120 Hz) ppm that were too broad for accurate integration.

X-ray Crystallography of 2 and 4. Data for **2** and **4** were collected on a CAD4 diffractometer with graphite monochromatized Mo Kα radiation (λ = 0.710 73 Å) at 153 K. In all structures, three check reflections were measured every 3 h and showed no significant intensity variation. The data were corrected for Lorenz effects and polarization. Absorption effects were corrected for by the empirical ψ-scan method. The structures were solved by Patterson and direct methods (SHELXS-86).[12] All non-hydrogen atoms were refined (SHELXL93)[13] based upon F_{obs}^2. All hydrogen atom coordinates were calculated with idealized geometries (SHELXL93). Crystallographic data and final R indices for **2** and **4** are given in Table 1. Significant bond distances and angles for **2** and **4** are given in Tables 2 and 3, respectively. Complete crystallographic details are given in the supplemental material.

Results and Discussion

Synthesis. Ln/Hg amalgams reduce diphenyl diselenide cleanly in THF and, if the reaction product is dissolved in pyridine, Ln(SePh)$_3$(pyridine)$_3$ (Ln = Ho (**1**), Tm (**2**), Yb (**3**)) can be isolated by crystallization in 70−90% yield. If the stoichiometry is precise, and if the chosen lanthanide can only form trivalent complexes, then the only soluble reaction products are lanthanide tris(benzeneselenolates). The tris(selenolate) compounds are moderately soluble in THF and conveniently soluble in pyridine, from which they can be crystallized by layering the solution with diethyl ether. Using this amalgam reaction, the tris(selenolates) of Tm, Ho, and Yb have been prepared.

Problems with this reaction should only be encountered for Ln = Eu or Yb, which can form divalent complexes. The Eu chemistry is relatively straightforward: Eu(SePh)$_3$ is unstable with respect to formation of Eu(II) and diphenyl diselenide,[5d] and so attempted preparations of Eu(SePh)$_3$ from an amalgam reaction will instead give the heterometallic chalcogenolate $[(THF)_3EuHg(SePh)_4]_2$.[14] The ytterbium chemistry is more complex. Structural characterization of (pyridine)$_4$LiYb(SePh)$_4$ proved that benzeneselenolate anions were sufficiently electronegative to function as the only anionic ligands in Yb(III) chemistry,[5c] but recent experiments have shown that when benzeneselenolate anions are the only anions present in a system, Hg will reduce Yb(III) in THF, and the resulting Hg(SePh)$_2$ reacts with Yb(SePh)$_2$ to form a heterometallic chalcogenolate complex.[15] Therefore, the use of only a catalytic amount of

Table 1. Crystal Data and Structure Refinement for **2** and **4**[a]

compd	$[(py)_3Tm(SePh)_3]_2$	$(py)_3Yb(SPh)_3$
empirical formula	$C_{71}H_{65}N_7Se_6Tm_2$	$C_{35.5}H_{32.5}N_{3.5}S_3Yb$
fw	913.96	777.37
space group	$P\bar{1}$	$P\bar{1}$
a (Å)	10.435(2)	9.836(10)
b (Å)	12.748(2)	11.304(14)
c (Å)	14.453(2)	16.202(11)
α (deg)	69.85(2)	80.70(8)
β (deg)	80.71(2)	77.91(7)
γ (deg)	69.03(2)	68.34(9)
vol (Å^3)	1683.8(5)	1630(3)
Z	2	2
density (calcd) (Mg/m^3)	1.803	1.584
temp (K)	153(2)	153(2)
λ (Å)	0.710 73	0.710 73
abs coeff (mm^{-1})	5.907	3.091
no. of obsd reflcns	5027	4457
final $R(F_o)$ [I > 2σ]	0.0260	0.0376
wR(F_o^2) indices [I > 2σ]	0.0649	0.1224

[a] Definitions: $R(F_o) = S||F_o| - |F_c||/S|F_o|$. $wR(F_o^2) = \{\sum[w(F_o^2 - F_c^2)^2]/\sum[w(F_o^2)^2]\}^{1/2}$. Additional crystallographic details are given in the supplemental material.

Table 2. Significant Bond Lengths (Å) and Angles (deg) for **2**[a]

Tm(1)−N(2)	2.429(3)	Tm(1)−N(1)	2.474(3)
Tm(1)−N(3)	2.489(4)	Tm(1)−Se(3)	2.8264(7)
Tm(1)−Se(2)	2.8364(9)	Tm(1)−Se(1)	2.9301(8)
Tm(1)−Se(1)′	2.9757(7)	Se(1)−Tm(1)′	2.9756(7)
N(2)−Tm(1)−N(1)	83.77(12)	N(2)−Tm(1)−N(3)	146.60(11)
N(1)−Tm(1)−N(3)	85.24(12)	N(2)−Tm(1)−Se(3)	79.91(8)
N(1)−Tm(1)−Se(3)	90.87(8)	N(3)−Tm(1)−Se(3)	68.83(8)
N(2)−Tm(1)−Se(2)	101.01(9)	N(1)−Tm(1)−Se(2)	172.84(8)
N(3)−Tm(1)−Se(2)	93.42(9)	Se(3)−Tm(1)−Se(2)	95.20(3)
N(2)−Tm(1)−Se(1)	136.53(8)	N(1)−Tm(1)−Se(1)	90.97(8)
N(3)−Tm(1)−Se(1)	74.98(8)	Se(3)−Tm(1)−Se(1)	143.47(2)
Se(2)−Tm(1)−Se(1)	81.89(3)	N(1)−Tm(1)−Se(1)′	85.25(8)
N(3)−Tm(1)−Se(1)′	137.37(8)	Se(3)−Tm(1)−Se(1)′	152.70(2)
Se(2)−Tm(1)−Se(1)′	91.04(2)	Se(1)−Tm(1)−Se(1)′	63.74(2)
C(1)−Se(1)−Tm(1)	115.37(12)	C(1)−Se(1)−Tm(1)′	114.94(12)

[a] Symmetry transformations used to generate equivalent primed atoms: $-x + 1, -y + 1, -z - 2$.

Table 3. Significant Bond Lengths (Å) and Angles (deg) for **4**

Yb−S(1)	2.682(3)	Yb−N(1)	2.445(6)
Yb−S(2)	2.650(2)	Yb−N(2)	2.459(6)
Yb−S(3)	2.609(4)	Yb−N(3)	2.449(6)
N(1)−Yb−N(3)	82.1(2)	N(1)−Yb−N(2)	173.2(2)
N(3)−Yb−N(2)	91.7(2)	N(1)−Yb−S(3)	81.6(2)
N(3)−Yb−S(3)	162.01(14)	N(2)−Yb−S(3)	104.9(2)
N(1)−Yb−S(2)	91.6(2)	N(3)−Yb−S(2)	87.8(2)
N(2)−Yb−S(2)	90.9(2)	S(3)−Yb−S(2)	85.23(9)
N(1)−Yb−S(1)	88.1(2)	N(3)−Yb−S(1)	80.4(2)
N(2)−Yb−S(1)	88.2(2)	S(3)−Yb−S(1)	106.45(9)
S(2)−Yb−S(1)	168.12(5)	C(1)−S(1)−Yb	101.8(2)
C(7)−S(2)−Yb	112.6(2)	C(13)−S(3)−Yb	97.9(2)

(11) *Ref. Natl. Bur. Stand., Monogr. (U.S.)* **1967**, *25*, Sect 5.
(12) Sheldrick, G. M. SHELXS86, Program for the Solution of Crystal Structures, University of Gottingen, Germany, 1986.
(13) Sheldrick, G. M. SHELXL-93, Program for Crystal Structure Refinement, University of Gottingen, Germany, 1993.
(14) Berardini, M.; Emge, T. J.; Brennan, J. G. *J. Am. Chem. Soc.* **1994**, *116*, 6941−2.

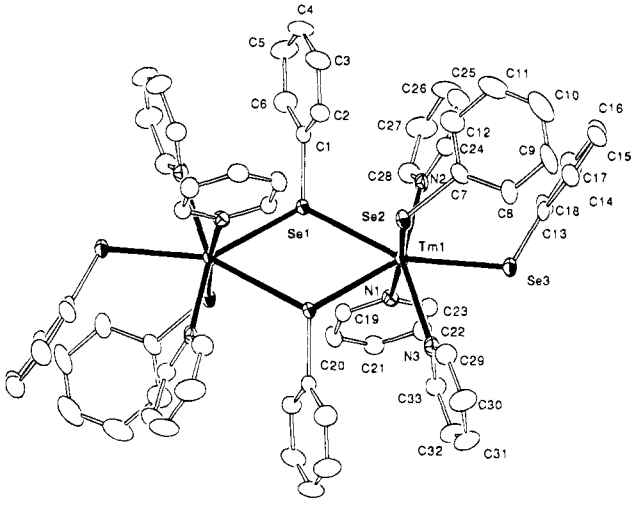

Figure 1. Molecular structure of $[(pyridine)_3Tm(SePh)_3]_2$. The complex is dimeric in the solid state, with a pair of μ_2-selenolate ligands bridging the seven coordinate pentagonal biypramidal Tm(III) ions. Significant distances (Å): Tm−N(avg), 2.46(2); Tm(1)−Se(3), 2.8264(7); Tm-(1)−Se(2), 2.8364(9); Tm(1)−Se(1), 2.9301(8); Tm(1)−Se(1)′, 2.9757-(7).

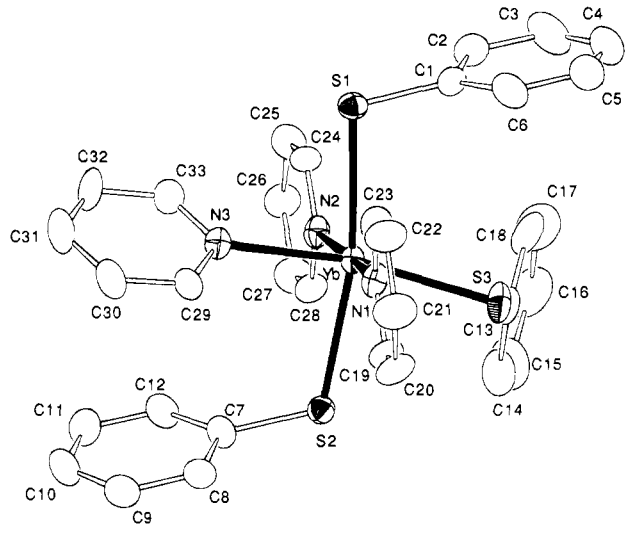

Figure 2. Molecular structure of *mer*-$(pyridine)_3Yb(SPh)_3$. The octahedral complex has inequivalent Yb−S bonds, with the Yb−S bond *trans* to a pyridine ligand being shorter than the Yb−S bonds *trans* to a thiolate. The Yb−N distances are statistically equivalent. Significant distances (Å): Yb−N(av), 2.451(4); Yb−S(3), 2.609(4); Yb−S(2), 2.650(2); Yb−S(1), 2.682(3).

mercury is crucial to the successful synthesis of $Yb(SePh)_3$ coordination complexes. It should be noted that while Sm also has a chemically accessible divalent oxidation state, Hg does not reduce $Sm(SePh)_3$.[14]

In order to establish whether this amalgam reaction would also work in thiolate chemistry, PhSSPh was reduced with Yb/Hg. Again, only a small amount of Hg is necessary for the reaction to proceed to completion. The final reaction product is moderately soluble in THF but dissolves readily in pyridine and can be crystallized as the pyridine coordination complex $(pyridine)_3Yb(SPh)_3$ (**4**).

The optical properties of the redox active Yb complexes are distinct from those of **1** and **2**, in which the metal has only a single chemically accessible oxidation state. Both ytterbium compounds are intensely colored due to a chalcogen to ytterbium charge transfer (CT) excitation. The CT excitation in the thiolate complex **4** is higher in energy than the corresponding absorption energy in **3** (λ_{max} = 510 nm for **3**; λ_{max} = 470 nm for **4**), but the concentration dependence of the selenolate spectrum and the absence of a significant concentration dependence in the thiolate spectrum prohibits an interpretation of the energy differences in terms of simple chalcogen substitution. As the concentration of **3** is increased, the position of the CT band shifts to higher energy. The optical concentration dependence is consistent with the monomeric structure of **4** and the dimeric structure of **3**.

Structure. The molecular structures of **2** and **4** were determined by low temperature single-crystal X-ray diffraction. Table 2 gives a listing of significant bond lengths and angles for **2**, which is a dimer in the solid state with a pair of 7-coordinate Tm(III) ions bridged by a pair of μ_2-benzeneselenolates. The metal coordination sphere is a trigonal bipyramid, with one pyridine and one benzeneselenolate in the axial positions. The difference between terminal and bridging Tm−Se bond lengths in **2** (0.10 Å) is comparable to the difference between terminal Sm−Se bonds and the Sm−Se bonds to Se atoms that bridge the seven coordinate Sm(III) ions in $(pyridine)_4SmNa(SePh)_5$ (0.11 Å).[15] In comparison, Ln−Se bonds to selenolates that bridge to smaller, less highly charged alkali metals are not lengthened as significantly. In $(pyridine)_4YbLi(SePh)_4$, the difference between terminal and bridging Yb−Se bonds is 0.05 Å[5c] and in $(pyridine)_4SmNa(SePh)_5$ the Sm−Se bonds to Se atoms are 0.07 Å longer than the terminal Sm−Se bond. A lengthening of the bridging Tm−Se bond in **2** relative to those in $(pyridine)_4YbLi(SePh)_4$ reduces interligand repulsive interactions, and this is presumably what permits adoption of a 7-coordinate structure, rather than the octahedral geometry in the YbLi complex. The slightly larger ionic radius of Tm (0.01 Å[16]) also helps to stabilize the 7-coordinate geometry.

In contrast to the selenolate dimer, **4** is a meridional octahedral molecular complex. Table 3 gives a listing of significant bond lengths and angles for **4**. The smaller coordination number in **4** can be attributed to ligand−ligand repulsive interactions. Short Yb−S bonds lessen the distances between the phenyl groups and other ligands, thus increasing repulsive interactions and leading to a 6-coordinate compound. Such reasoning was used to explain the differing coordination numbers of $(pyridine)_4Yb(SePh)_2$ and $(pyridine)_5Yb(TePh)_2$, where the larger (by 0.23 Å) Te atom distances the phenyl group from the metal coordination sphere, again decreasing interligand repulsions and permitting the coordination of an additional pyridine ligand.[5f]

Molecular **4** has two types of phenylthiolate and two types of pyridine coordination sites, and there appears to be a small but significant difference in the length of Yb−S bonds *trans* to thiolate ligands (Yb−S(2), 2.650(2)Å; Yb−S(1), 2.682(3)Å), relative to the Yb−S bond *trans* to pyridine (Yb−S(3), 2.609-(4)). There are no statistically significant differences in the Yb−N bond lengths. Similar inequivalent Yb−S bonds (and equivalent Yb−N bonds) are also present in the structures of *mer*-$(L)_3Ln(S\text{-}2,4,6\text{-}^{i}pr\text{-}C_6H_3)_3$. (L = py, Ln = Sm; L = py/THF, Ln = Yb).[5j]

In lanthanide chemistry, bond lengths can usually be accurately predicted by the summation of ionic radii. While this bonding model works well with most ligand systems, in chalcogenolate chemistry there are deviations from ideal bond length behavior. We can compare the bond lengths in **4** with related bonds in $(pyridine)_4Yb(SPh)_2$, (Yb−S, 2.827(3) Å;

(15) Berardini, M.; Emge, T. J.; Brennan, J. G. Submitted to *J. Am. Chem. Soc.*

(16) Shannon, R. D. *Acta Crystallogr. A*, **1976**, *32*, 751.

average Yb–N, 2.55 Å)[5f] to evaluate how metal oxidation state influences bonds from Yb to sulfur and nitrogen. According to ionic radius bonding models, a change in metal oxidation state should change all the metal–ligand bond lengths by an equal amount. Shannon's tables list a difference between Yb(II) and Yb(III) ionic radii of 0.15 Å (for coordination number = 6), and in the two benzenethiolate structures, there is a difference of 0.18 Å in Yb–S bond lengths and 0.10 Å in Yb–N bond lengths. Similar deviations from ideal bond length behavior were noted previously in the comparison of $(pyridine)_4Yb(SePh)_2$ with $(pyridine)_4YbLi(SePh)_4$, and in an analysis of isostructural $[Cp^*_2Sm]_2$–E structures.[3f] In divalent chalcogenolate chemistry ionic radii can still be used to accurately predict metal–ligand bond lengths to within 0.01 Å.[5f]

Thermolysis. Because these molecules were prepared for subsequent doping of chalcogenide matrices and because we are interested in using these molecules as starting materials in the synthesis of nanometer-sized lanthanide–chalcogenide clusters, it was important to establish what solid state phases would result from thermal decomposition reactions. While there have been a number of examples showing that divalent lanthanide chalcogenolate precursors ($Ln(ER)_2$) decompose to give LnE (E = Se, Te) solids,[5a,g,15] in trivalent chemistry only the decomposition of $Ce(TeR)_3$ to give Ce_2Te_3 has been reported.[5b] In all cases, thermolysis involved the well-documented[17] elimination of volatile R_2E products.

Heating samples of **1**–**3** initially results in the dissociation of pyridine, which condenses in the part of the tube extended outside of the furnace. Further heating results in the evolution of Ph_2Se, which was identified by a characteristic ^1H NMR spectrum. The thermolyses are complete by the time the sample temperature is raised to 300 °C—no further volatile products are observed above this temperature. The final solid state products were then further annealed at 1000 °C to insure sample crystallinity, and the final solid state powders were examined by X-ray powder diffraction. Reactions 1, 2, and 3 describe the results of the thermolysis reactions.

$$Ho(SePh)_3 \rightarrow HoSe + HoSe_2 + Ph_2Se \quad (1)$$

$$Tm(SePh)_3 \rightarrow Tm_2Se_3 + Ph_2Se \quad (2)$$

$$Yb(SePh)_3 \rightarrow Yb_2Se_3 + Ph_2Se \quad (3)$$

Thermolysis of the thulium precursor **2** gives Tm_2Se_3, which is essentially a rock salt structure with metal vacancies.[10] This is the expected solid state phase according to the reported phase diagram.[18] In contrast, thermolysis of the holmium compound leads to the formation of HoSe and $HoSe_2$. This phase separation may be understood in the context of known $HoSe_x$ chemistry: Ho_2Se_3 will eliminate Se to give $HoSe_{1.4}$ at 1500 °C under vacuum,[19] and $HoSe_2$ can been isolated from Se rich environments if the temperature is kept below 800 °C.[9] Because the thermolysis of **2** is essentially complete at 300 °C and the sample is annealed at relatively low temperatures, metastable $HoSe_2$ can be identified as a reaction product. Thermolysis of this precursor molecule in solution should lead to interesting nanocluster chemistry.

Thermolysis of of the Yb precursor **3** was particularly interesting because the metal is redox active. In principle, $Yb(SePh)_3$ could decompose to give either Yb_2Se_3 and Ph_2Se or YbSe, Ph_2Se, and Ph_2Se_2. Both metal chalcogenides are stable solid state phases (Yb_2Se_3 will eliminate Se at elevated temperatures, but it is stable under vacuum at temperatures as high as 1150 °C[20]) and so the final solid state product is dependent on the relative kinetics of diphenyl diselenide reductive elimination and diphenyl monoselenide evolution. In the chemistry of the redox active lanthanide chalcogenolates, reductive elimination has considerable precedent: in phenyltellurolate chemistry, Yb(III) eliminates Ph_2Te_2 to form $Yb(TePh)_2$ coordination complexes at room temperature,[5e] and in selenolate chemistry $Eu(SePh)_3$ is unstable with respect to elimination of Ph_2Se_2 and the formation of $Eu(SePh)_2$ coordination complexes.[5d] Thermolysis of **3** shows that reductive elimination does not occur. As found for complexes **1** and **2**, **3** decomposes by first losing coordinated pyridine, and this is followed by the evolution of Ph_2Se—at no time is there any evidence for the formation of PhSeSePh. X-ray powder diffraction confirms that Yb_2Se_3 is present as the only crystalline product in the thermolysis of **3**.

Conclusions

Lanthanide tris(benzeneselenolates) can be conveniently prepared in high yield by the direct reduction of Ph_2Se_2 with Ln/Hg amalgams—the generality of this reaction for redox-active and nonredox-active metals was established by preparing Ho, Tm, and Yb compounds. The tris(benzeneselenolates) can be isolated as pyridine coordination complexes, and single-crystal X-ray characterization of the Tm compound revealed a 7-coordinate dimeric structure. Thermolysis of the selenolate complexes give a variety of solid state phases, including LnSe, Ln_2Se_3, and metastable $LnSe_2$. The molecular thiolate $(pyridine)_3Yb(SPh)_3$ was also synthesized and characterized to demonstrate the utility of this amalgam reaction in lanthanide thiolate syntheses.

Acknowledgment. We thank Dr. T. J. Emge for assistance with the single crystal X-ray diffraction work and Dr. Jonggyu Lee for help with the powder X-ray diffraction experiments. This work was supported by the National Science Foundation under Grant No. CHE-9204160.

Supplementary Material Available: X-ray powder diffraction patterns of thermolysis products of **1**-**3** and tables of crystallographic details and refinement results for **2** and **4** (13 pages). This material is contained in many libraries on microfiche, immediately follows this article in the microfilm version of the journal, and can be ordered from the ACS; see any current masthead page for ordering information.

IC950035D

(17) (a) Osakada, K.; Yamamoto, A. *Inorg. Chem.* **1990**, *30*, 2328. (b) Osakada K.; Yamamoto, T. *J. Chem. Soc., Chem. Commun.* **1987**, 1117. (c) Steigerwald, M.; Sprinkel, C. *J. Am. Chem. Soc.* **1987**, *109*, 7200. (d) Brennan, J.; Siegrist, T.; Carroll, C.; Stuczynski, S.; Brus, L.; Steigerwald, M *J. Am. Chem. Soc.* **1989**, *111*, 4141. (e) Brennan, J.; Siegrist, T.; Stuczynski, S.; Carroll, C.; Rynders, P.; Brus, L.; Steigerwald, M. *Chem. Mater.* **1990**, *2*, 403. (f) Kern, R. J. *J. Am. Chem. Soc.* **1953**, *75*, 1865. (g) Peach, M. E. *J. Inorg. Nucl. Chem.* **1973**, *35*, 1046. (h) Peach, M. E. *J. Inorg. Nucl. Chem.* **1979**, *41*, 1390. (i) Craig, D.; Dance, I.; Garbutt, R. *Angew. Chem., Int. Ed. Engl.* **1986**, *25*, 165. (j) Dance, I.; Garbutt, R.; Craig, D.; Scudder, M. *Inorg. Chem.* **1987**, *26*, 4057.

(18) Kaldis, E.; Spychiger, H.; Jilek, E. *J. Magn. Magn. Mater.* **1985**, *47/48*, 478–480.

(19) Guittard, M.; Flahaut, J.; Lepeltier, M. *Bull. Soc. Chim. Fr.* **1968**, 4759–4765.

(20) Pawlak, L.; Duczmal, M.; Pokrzywinicki, S.; Czopnik, A. *Solid State Commun.* **1980**, *34*, 195–197.